Journal of Biosciences and Medicines, 2026, 14(6), 385-403
https://www.scirp.org/journal/jbm
ISSN Online: 2327-509X
ISSN Print: 2327-5081

Bioinformatics Analysis of the Expression Characteristics, Clinical Associations, and Prognostic Value of SLC7A11 in Glioma

Jiayuan Zhang[1,2], Zongquan Nie[2], Ruijie Zheng[3], Yuxuan Li[3], Chuanyu Li[1*]

[1]Department of Neurosurgery, Affiliated Hospital of Youjiang Medical University for Nationalities, Baise, China
[2]Graduate School, Youjiang Medical University for Nationalities, Baise, China
[3]College of Clinical Medical, Youjiang Medical University for Nationalities, Baise, China
Email: *793962178@qq.com

How to cite this paper: Zhang, J.Y., Nie, Z.Q., Zheng, R.J., Li, Y.X. and Li, C.Y. (2026) Bioinformatics Analysis of the Expression Characteristics, Clinical Associations, and Prognostic Value of SLC7A11 in Glioma. *Journal of Biosciences and Medicines*, **14**, 385-403.
https://doi.org/10.4236/jbm.2026.146026

Received: May 26, 2026
Accepted: June 23, 2026
Published: June 26, 2026

Copyright © 2026 by author(s) and Scientific Research Publishing Inc.
This work is licensed under the Creative Commons Attribution International License (CC BY 4.0).
http://creativecommons.org/licenses/by/4.0/

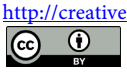

Open Access

Abstract

Objective: This study aims to investigate the expression characteristics, clinical prognostic value, and association with the tumor immune microenvironment of solute carrier family 7 member 11 (SLC7A11) in glioma through bioinformatics analysis, and to construct a nomogram prediction model based on key clinicopathological variables and SLC7A11 expression levels. The findings provide a theoretical basis for revealing the potential involvement of SLC7A11 in ferroptosis, immune regulation, and metabolic reprogramming during glioma progression, enrich the evidence for SLC7A11 as a potential biomarker in glioma, and offer candidate molecular targets for future immune-metabolism-related intervention strategies. **Methods:** Transcriptomic data and corresponding clinical information of glioma and normal brain tissues were obtained from the TCGA and GTEx databases. Glioma patients were divided into high- and low-expression groups based on the median expression level of SLC7A11. Chi-square tests were used to compare differences in clinical characteristics, including WHO grade, age, histological type, and survival event rates, between the two groups. GO and KEGG enrichment analyses as well as GSEA were performed to evaluate biological pathways associated with SLC7A11 expression. The ssGSEA algorithm was employed to calculate the infiltration abundances of 24 immune cell types, and Spearman correlation analysis was conducted to examine the relationship between SLC7A11 expression and immune cell infiltration levels. Kaplan–Meier curves were generated for overall survival (OS), disease-specific survival (DSS), and progression-free interval (PFI), and the log-rank test was used to assess between-group differences. Stratified survival analyses based on LGG, GBM, and IDH classification were not performed in this study, and relevant subgroup validation will be addressed in future research. Univariate and multivariate Cox regression models

were applied to analyze the independent prognostic value of SLC7A11 and other clinical variables. A nomogram prediction model integrating WHO grade, IDH status, age, and SLC7A11 expression was constructed, and its predictive accuracy for 1-, 3-, and 5-year survival probabilities was evaluated by calibration curves. **Results:** SLC7A11 expression levels were significantly higher in a variety of tumor tissues than in normal brain tissue. After stratifying glioma patients by the median SLC7A11 expression level, the high-expression group showed a lower WHO grade, younger age, fewer cases of glioblastoma, and a lower rate of overall survival events (all $P < 0.05$). Functional enrichment analysis of differentially expressed genes revealed that the high SLC7A11 expression group was significantly enriched in the bile acid metabolism pathway and the KRAS signaling downregulation pathway, whereas the low-expression group was enriched in cell cycle-related pathways (such as E2F targets and G2/M checkpoint) and pro-cancer-related pathways such as epithelial–mesenchymal transition (EMT). Immune infiltration analysis demonstrated that the SLC7A11 expression level was significantly positively correlated with the infiltration abundances of follicular helper T cells (TFH), central memory T cells (Tcm), and $\gamma\delta$ T cells (Tgd), and significantly negatively correlated with Th2 cells. Survival analysis showed that patients in the high SLC7A11 expression group had significantly better OS, DSS, and PFI than those in the low-expression group (log-rank test $P < 0.05$ for all). Multivariate Cox regression analysis indicated that SLC7A11 expression was not an independent prognostic factor for OS in glioma patients. Nevertheless, the nomogram constructed based on WHO grade, IDH status, age, and SLC7A11 expression demonstrated good consistency between the predicted 1-, 3-, and 5-year survival probabilities and the actual observations, as shown by calibration curves. **Conclusion:** SLC7A11 is expressed at a high level in glioma, and its high expression is significantly associated with a lower WHO grade, a non-glioblastoma phenotype, and longer overall survival. This association challenges the conventional view that SLC7A11 serves as an adverse prognostic marker in most solid tumors. Functional enrichment suggested that the high-expression group was enriched in bile acid metabolism and KRAS signaling downregulation, whereas the low-expression group exhibited activation of EMT and cell cycle pathways. Immune infiltration analysis revealed that SLC7A11 was positively correlated with TFH, Tcm, and Tgd, and negatively correlated with Th2 cells. Although not an independent prognostic factor, the nomogram model incorporating SLC7A11 showed good predictive performance and may serve as a potential complementary marker for prognostic assessment in glioma.

Keywords

Glioma, SLC7A11, Prognostic Analysis, Tumor Immune Microenvironment, Bioinformatics Analysis

1. Introduction

Glioma is the most common primary malignant tumor of the central nervous sys-

tem, exhibiting highly heterogeneous biological behavior ranging from relatively indolent low-grade glioma (LGG) to highly aggressive glioblastoma (GBM), forming a continuous disease spectrum. Globally, the annual incidence of glioma is approximately 5 - 6 per 100,000 persons, with GBM accounting for more than half. Despite advances in multimodal comprehensive treatment-including surgical resection, radiotherapy, and alkylating agent chemotherapy represented by temozolomide-patient prognosis remains extremely poor. The median survival of GBM patients is usually only 12 - 15 months, and the five-year survival rate is less than 5% [1]. The roots of this therapeutic dilemma lie in the inherent high invasiveness of glioma cells, primary and acquired resistance to radiotherapy and chemotherapy, and the immunosuppressive state mediated by the complex tumor microenvironment composed of tumor cells, stromal cells, and immune cells. Therefore, in-depth elucidation of the molecular mechanisms underlying glioma development, and identification of new reliable prognostic biomarkers and therapeutic targets, are of urgent clinical significance for achieving precise stratification of glioma and improving patient outcomes.

Among many potential molecular targets, solute carrier family 7 member 11 (SLC7A11) has attracted considerable attention due to its central role in regulating cellular redox homeostasis and programmed cell death. SLC7A11 encodes the key subunit of the cystine/glutamate antiporter xCT, responsible for transporting extracellular cystine into the cell for glutathione (GSH) synthesis. GSH is a major defense against oxidative stress and lipid peroxidation damage. Consequently, SLC7A11 is recognized as a key negative regulator of ferroptosis; its high expression effectively inhibits ferroptosis and promotes tumor cell survival. Existing studies have confirmed that SLC7A11 is widely overexpressed in various solid tumors and is significantly associated with poor patient prognosis [2]. For example, in renal cell carcinoma, high SLC7A11 expression not only predicts worse survival but also promotes tumor progression by inhibiting ferroptosis and inducing metabolic reprogramming [3]. Similarly, in lung adenocarcinoma and colorectal cancer, SLC7A11 overexpression has been confirmed to be associated with malignant progression, treatment resistance, and poor prognosis [4] [5]. These findings collectively demonstrate a clear oncogenic function of SLC7A11.

However, in glioma, the biological function and clinical significance of SLC7A11 present a more complex and multifaceted picture. On one hand, mechanistic studies have confirmed its critical role in glioma cells, revealing that its expression is finely regulated by various signaling axes such as PI3K/AKT/HIF-1α and AMPKα1-ZDHHC8 [1] [6]. These studies show that SLC7A11 resists ferroptosis by stabilizing proteins or enhancing their function, thereby maintaining the stemness of glioma stem cells and tumor growth [7] [8]. Moreover, it has been reported that IDO1 upregulates SLC7A11 mRNA stability via FTO-dependent m6A methylation, thereby inhibiting ferroptosis and promoting GBM progression [9]. On the other hand, analyses of public databases have revealed conclusions contrary to pan-cancer studies. This inconsistency between molecular function and clinical

association suggests that the role of SLC7A11 in the glioma immune microenvironment may be particularly unique; its high expression may not directly drive malignant proliferation but rather be associated with a relatively low-grade malignant molecular subtype or a distinct immune state.

Systematic evaluation of SLC7A11 expression landscape, prognostic value, and interaction with the tumor immune microenvironment in glioma is of great theoretical importance and potential clinical translational value for bridging the above-mentioned cognitive divergence and revealing its true mechanism in glioma development. Although some studies have preliminarily explored the association between SLC7A11 and immune infiltration in glioma, most are limited to a single perspective of ferroptosis or disulfide stress, lacking a comprehensive multi-omics integration from expression characteristics, functional pathways, to immune microenvironment [10] [11]. Furthermore, studies constructing clinical prognostic prediction models based on SLC7A11 are still relatively scarce, limiting its potential as a clinical decision-support tool. Therefore, this study aims to use large-scale transcriptomic and clinical data from The Cancer Genome Atlas (TCGA) and Genotype-Tissue Expression (GTEx) databases, through systematic bioinformatics analysis, to elucidate the expression patterns, clinicopathological associations, and prognostic value of SLC7A11 in glioma from multiple dimensions.

2. Materials and Methods

2.1. Data Sources and Processing

Glioma mRNA transcriptome and corresponding clinical data (including WHO pathological grade, IDH mutation, histological classification, sex, age, race, and survival outcomes) were downloaded from the TCGA database (https://portal.gdc.cancer.gov/), which provides three types of normalized transcriptomic data: TPM, FPKM, and RPM. Normal brain tissue transcriptomic data were obtained through the UCSC Xena platform using the GTEx v8 dataset, comprising a total of 1,646 normal samples from multiple brain regions. This study enrolled 699 TCGA glioma cases, which were dichotomized into low-expression (n = 349) and high-expression (n = 350) groups based on the median SLC7A11 expression level. The R package sva was applied to perform cross-dataset batch correction between TCGA tumor and GTEx normal samples, and all samples were uniformly standardized to TPM format for subsequent analyses. Various degrees of missing data were present across clinical indicators. In the clinicopathological comparison, WHO grade was missing in 62 cases, IDH status in 10 cases, age and sex information in a total of 1 case, and race data in 13 cases; Cox regression analyses used complete cases with available survival data, resulting in slightly different sample sizes across variables. Chi-square tests, logistic regression, and Cox regression all employed the complete-case method to handle missing data. In univariate analyses, cases with missing values for the corresponding indicator were excluded, and multivariate regression included only samples with complete data for all covariates, resulting in differing total sample sizes across statistical tables.

2.2. Study Grouping and Expression Analysis

Glioma patients were divided into high- and low-expression groups according to the median SLC7A11 expression level. Boxplots were used to display SLC7A11 expression differences across 33 cancer types and in glioma, and the Wilcoxon rank-sum test was used to compare expression levels between tumor and normal tissues.

2.3. Association with Clinicopathological Characteristics

Chi-square tests were used to compare differences in clinicopathological characteristics between the SLC7A11 high- and low-expression groups, including WHO grade, IDH status, histological type, sex, age, race, and OS event. Binary logistic regression analysis was further performed to examine the association between each clinical characteristic and SLC7A11 expression level, with the strength of association expressed as odds ratios (OR) and 95% confidence intervals (CI). Histological type was classified according to clinical standards into glioblastoma (GBM) and non-glioblastoma (astrocytoma, oligoastrocytoma, and oligodendroglioma), with GBM serving as the reference group in logistic regression for ease of clinical interpretation.

2.4. Differential Expression Genes (DEGs) and Functional Enrichment Analysis

The DESeq2 package was used to analyze differentially expressed genes between the SLC7A11 high- and low-expression groups based on the HTSeq-Counts raw count data of TCGA glioma samples. The screening criteria were $|\log_2(\text{fold change})| > 1$ and adjusted P value (adj.P) < 0.05, and the distribution of DEGs was visualized with a volcano plot. Subsequently, Gene Ontology (GO) and Kyoto Encyclopedia of Genes and Genomes (KEGG) enrichment analyses were performed on the DEGs using the clusterProfiler package, with adj.P < 0.05 as the significance threshold for enrichment. Meanwhile, Gene Set Enrichment Analysis (GSEA) was conducted to explore Hallmark pathways associated with SLC7A11 expression, with the significance criteria defined as |normalized enrichment score (NES)| > 1, adj.P < 0.001, and false discovery rate (FDR) < 0.001.

2.5. Immune Microenvironment Correlation Analysis

Single-sample Gene Set Enrichment Analysis (ssGSEA) was used to calculate infiltration scores of 24 immune cell types in glioma patients. Spearman correlation analysis was performed to explore the relationship between SLC7A11 expression level and each immune cell infiltration score, with correlation coefficient (R) and P value indicating the strength of association. Bubble plots and scatter plots were used to visualize the correlation results.

2.6. Survival Analysis and Prognostic Model Construction

Kaplan-Meier curves were generated for OS, DSS, and PFI of patients in the

SLC7A11 high- and low-expression groups, and the log-rank test was used to compare survival differences between the groups. In this study, stratified survival analyses by WHO grade (LGG vs. GBM) and IDH status (mutant vs. wild-type) were not conducted within the current TCGA cohort; this stratified validation is planned to be performed in a subsequent independent clinical cohort. Univariate and multivariate Cox proportional hazards regression models were employed to identify prognostic factors influencing OS in glioma patients. Variables with $P < 0.1$ in the univariate analysis were included in the multivariate analysis, and the strength of association was expressed as hazard ratios (HR) with 95% confidence intervals (CI). Based on the multivariate Cox regression results, a nomogram integrating WHO grade, IDH status, age, and SLC7A11 expression level was constructed to predict the 1-, 3-, and 5-year OS probabilities. The predictive performance of the nomogram was evaluated by calibration curves, with the consistency between predicted and observed probabilities serving as an assessment of model accuracy.

2.7. Statistical Analysis

All data analyses were performed using R software (version 4.3.1). Continuous variables were expressed as mean ± standard deviation, and comparisons between groups were performed using t-tests or Wilcoxon rank-sum tests depending on data distribution. Significance criteria for differential gene screening were $|\log_2 FC| \geq 1$ and adjusted $P < 0.05$; for enrichment analysis, adjusted $P < 0.05$ was considered significant. All tests were two-sided, and $P < 0.05$ was considered statistically significant.

3. Results

3.1. Expression Characteristics of SLC7A11 in Pan-Cancer and Glioma

Pan-cancer expression analysis showed that SLC7A11 was significantly differentially expressed in multiple tumor types. Notably, its expression levels in low-grade glioma (LGG) and glioblastoma (GBM) were significantly higher than in normal brain tissue (**Figure 1**). SLC7A11 was also upregulated in breast cancer, cervical cancer, colon cancer, esophageal cancer, head and neck squamous cell carcinoma, liver cancer, lung cancer, pancreatic cancer, and other tumors, suggesting a broad role in tumor development.

3.2. Association between SLC7A11 Expression and Clinicopathological Characteristics of Glioma Patients

A total of 699 glioma patients were divided into high-expression (n = 350) and low-expression (n = 349) groups based on the median SLC7A11 expression level. Comparison of clinicopathological characteristics showed significant differences between the two groups in WHO grade, histological type, age, and OS event (all $P < 0.05$), whereas IDH status, gender, and race showed no significant differences

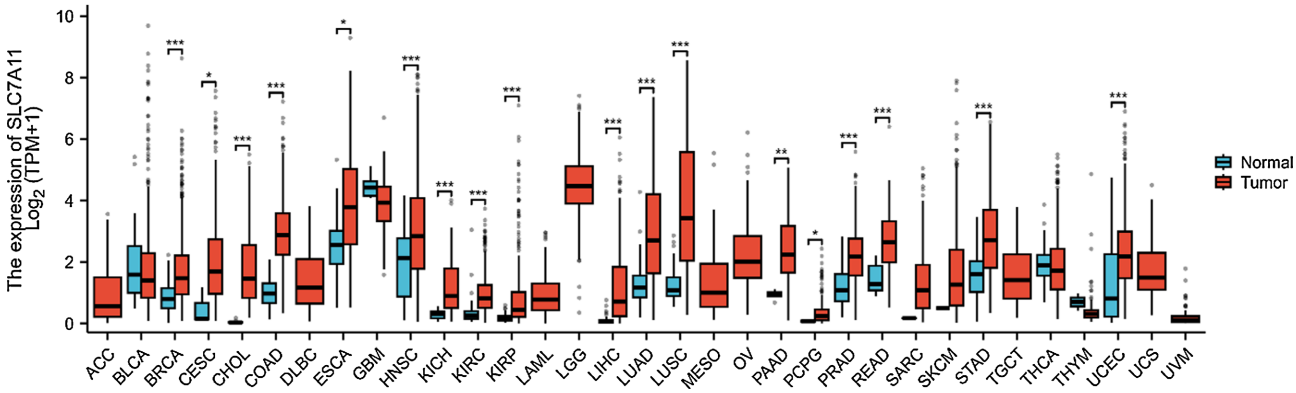

Figure 1. Expression characteristics of SLC7A11 in pan-cancer and glioma. Boxplot of SLC7A11 expression differences across pan-cancer and normal tissues.

(P > 0.05) (Table 1). Specifically, the low-expression group had a higher proportion of WHO grade G4 patients (37.4% vs. 15.4%), a higher proportion of glioblastoma (34.1% vs. 14%), a higher proportion of patients > 60 years old (23.5% vs. 17.4%), and a higher incidence of death events (44.1% vs. 33.7%). In contrast, the high-expression group had a higher proportion of WHO grade G2 patients (45.1% vs. 25.2%), higher proportions of astrocytoma and oligodendroglioma (31.1% vs. 24.9% and 31.7% vs. 25.5%, respectively), a higher proportion of patients ≤ 60 years old (82.6% vs. 76.5%), and a higher proportion of alive patients (66.3% vs. 55.9%).

Table 1. Comparison of clinicopathological characteristics between SLC7A11 high- and low-expression groups in glioma patients.

Characteristics	Low expression of SLC7A11	High expression of SLC7A11	P value
n	349	350	
WHO grade, n (%)			<0.001
G2	80 (25.2%)	144 (45.1%)	
G3	119 (37.4%)	126 (39.5%)	
G4	119 (37.4%)	49 (15.4%)	
IDH status, n (%)			0.273
WT	129 (37.7%)	117 (33.7%)	
Mut	213 (62.3%)	230 (66.3%)	
Histological type, n (%)			< 0.001
Astrocytoma	87 (24.9%)	109 (31.1%)	
Oligoastrocytoma	54 (15.5%)	81 (23.1%)	
Oligodendroglioma	89 (25.5%)	111 (31.7%)	
Glioblastoma	119 (34.1%)	49 (14%)	
Gender, n (%)			0.853

Continued

Female	150 (43%)	148 (42.3%)	
Male	199 (57%)	202 (57.7%)	
Age, n (%)			0.047
≤60	267 (76.5%)	289 (82.6%)	
>60	82 (23.5%)	61 (17.4%)	
Race, n (%)			0.169
Asian	9 (2.6%)	4 (1.2%)	
Black or African American	20 (5.8%)	13 (3.8%)	
White	315 (91.6%)	325 (95%)	
OS event, n (%)			0.005
Alive	195 (55.9%)	232 (66.3%)	
Dead	154 (44.1%)	118 (33.7%)	

Note: The original total number of cases was 699. Missing data were present in various clinical variables, and the complete-case method was adopted for the analysis, excluding samples with missing values for the corresponding indicator. Consequently, the Total (N) values differ across rows.

Further binary logistic regression analysis showed that WHO grade G4 (vs. G2 & G3, OR = 0.303, 95% CI: 0.208 - 0.444, P < 0.001) and age >60 years (vs. <= 60 years, OR = 0.687, 95% CI: 0.474 - 0.996, P = 0.047) were significantly associated with low SLC7A11 expression, whereas non-glioblastoma histology (including astrocytoma, oligoastrocytoma, and oligodendroglioma, vs. glioblastoma, OR = 3.178, 95% CI: 2.186 - 4.621, P < 0.001) was significantly associated with high SLC7A11 expression (Table 2), suggesting that low SLC7A11 expression is associated with a higher degree of malignancy in glioma.

Table 2. Logistic regression analysis of SLC7A11 expression level and clinicopathological characteristics.

Characteristics	Total (N)	OR (95% CI)	P value
WHO grade (G4 vs. G2 & G3)	637	0.303 (0.208 - 0.444)	<0.001
IDH status (Mut vs. WT)	689	1.191 (0.871 - 1.627)	0.273
Histological type (Astrocytoma & Oligoastrocytoma & Oligodendroglioma vs. Glioblastoma)	699	3.178 (2.186 - 4.621)	<0.001
Gender (Male vs. Female)	699	1.029 (0.762 - 1.388)	0.853
Age (>60 vs. ≤60)	699	0.687 (0.474 - 0.996)	0.047
Race (White vs. Asian & Black or African American)	686	1.760 (0.948 - 3.267)	0.073

Note: The original total number of cases was 699. Missing data were present in various clinical variables, and the complete-case method was adopted for the analysis, excluding samples with missing values for the corresponding indicator. Consequently, the Total (N) values differ across rows.

3.3. DEGs and Functional Enrichment Analysis between SLC7A11 High- and Low-Expression Groups

Differential expression analysis revealed a large number of DEGs between the SLC7A11 high- and low-expression groups. Significantly upregulated genes were mainly distributed in the high-expression group, while significantly downregulated genes were mainly in the low-expression group (Figure 2(a)). GO/KEGG enrichment analysis showed that DEGs were mainly enriched in immune-related pathways: molecular function (MF) was enriched in antigen binding and immunoglobulin receptor binding; cellular component (CC) was enriched in immunoglobulin complex; biological process (BP) was enriched in immunoglobulin production, phagocytosis recognition, and classical pathway of complement activation; KEGG pathways were enriched in systemic lupus erythematosus, alcoholism, and neutrophil extracellular trap formation (Figure 2(b)).

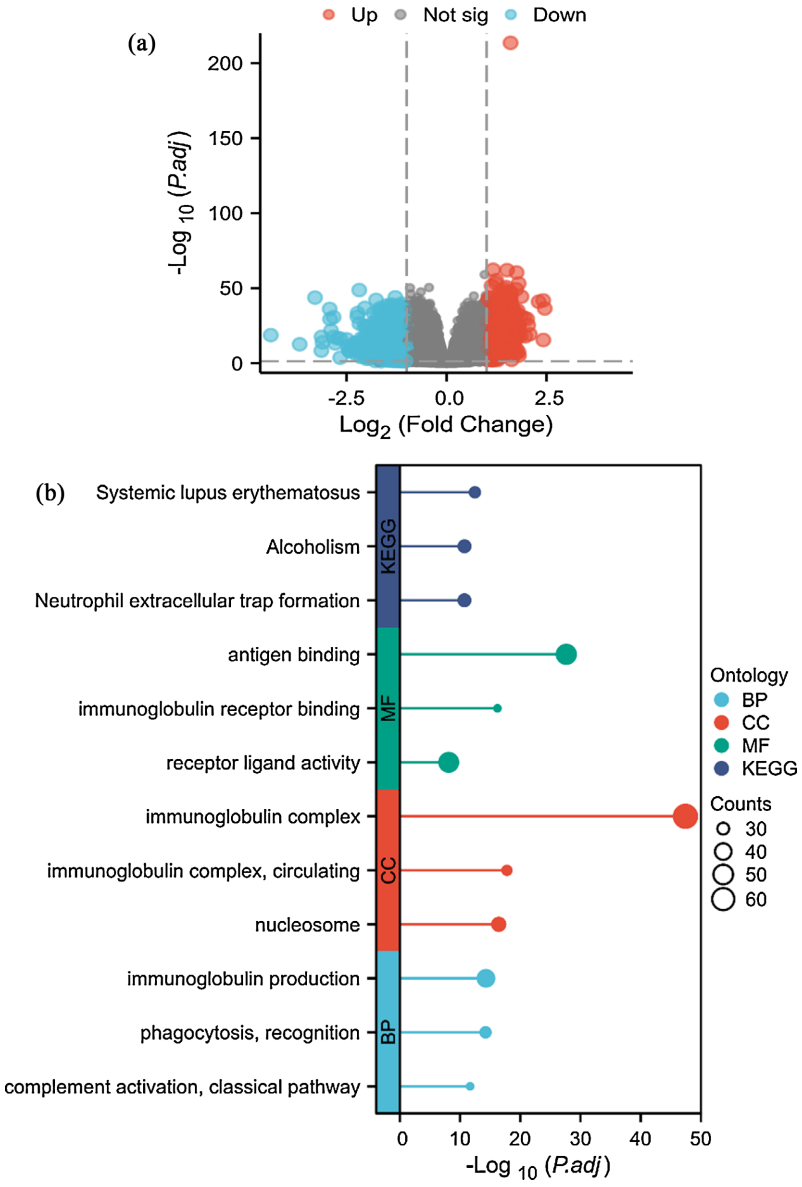

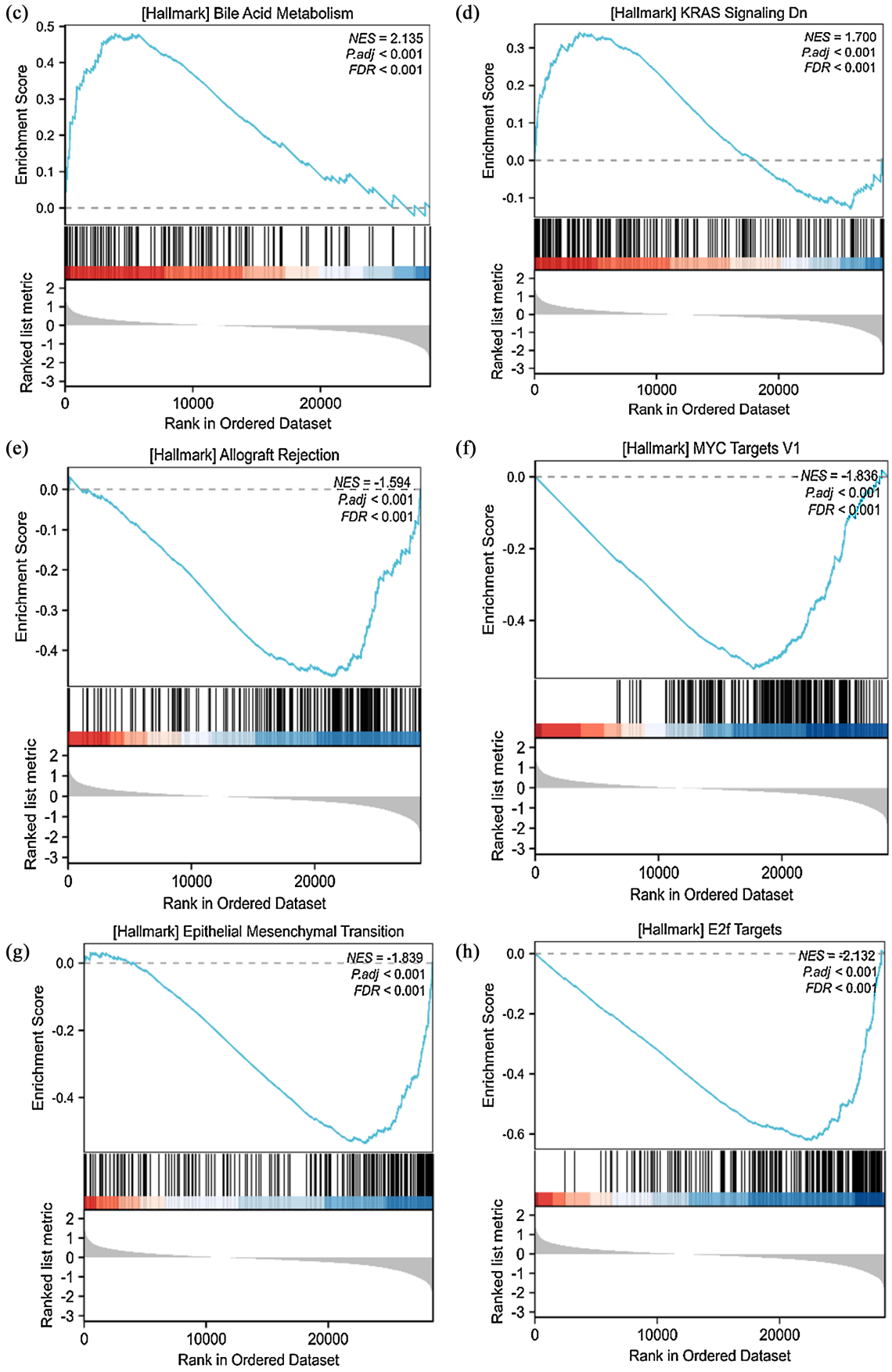
(c)
[Hallmark] Bile Acid Metabolism
NES = 2.135
P.adj < 0.001
FDR < 0.001
Enrichment Score
Ranked list metric
Rank in Ordered Dataset
(d)
[Hallmark] KRAS Signaling Dn
NES = 1.700
P.adj < 0.001
FDR < 0.001
Enrichment Score
Ranked list metric
Rank in Ordered Dataset
(e)
[Hallmark] Allograft Rejection
NES = -1.594
P.adj < 0.001
FDR < 0.001
Enrichment Score
Ranked list metric
Rank in Ordered Dataset
(f)
[Hallmark] MYC Targets V1
NES = -1.836
P.adj < 0.001
FDR < 0.001
Enrichment Score
Ranked list metric
Rank in Ordered Dataset
(g)
[Hallmark] Epithelial Mesenchymal Transition
NES = -1.839
P.adj < 0.001
FDR < 0.001
Enrichment Score
Ranked list metric
Rank in Ordered Dataset
(h)
[Hallmark] E2f Targets
NES = -2.132
P.adj < 0.001
FDR < 0.001
Enrichment Score
Ranked list metric
Rank in Ordered Dataset

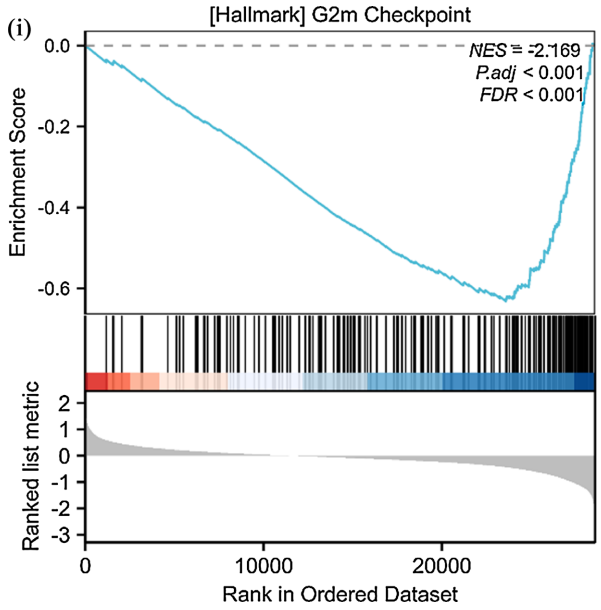

Figure 2. DEGs and functional enrichment analysis between SLC7A11 high- and low-expression groups. (a) Volcano plot of DEGs between SLC7A11 high- and low-expression groups; (b) GO/KEGG functional enrichment visualization; (c) GSEA enrichment curve for bile acid metabolism; (d) GSEA curve for KRAS signaling downregulation; (e) GSEA curve for allograft rejection; (f) GSEA curve for MYC targets V1; (g) GSEA curve for EMT; (h) GSEA curve for E2F targets; (i) GSEA curve for G2/M checkpoint.

GSEA results showed that the SLC7A11 high-expression group was significantly enriched in bile acid metabolism (NES = 2.135, adj.P < 0.001, FDR < 0.001) (**Figure 2(c)**) and KRAS signaling downregulation (NES = 1.700, adj.P < 0.001, FDR < 0.001) (**Figure 2(d)**); the low-expression group was significantly enriched in allograft rejection (NES = -1.594, adj.P < 0.001, FDR < 0.001) (**Figure 2(e)**), MYC targets V1 (NES = -1.836, adj.P < 0.001, FDR < 0.001) (**Figure 2(f)**), epithelial-mesenchymal transition (EMT, NES = -1.839, adj.P < 0.001, FDR < 0.001) (**Figure 2(g)**), E2F targets (NES = -2.132, adj.P < 0.001, FDR < 0.001) (**Figure 2(h)**), and G2/M checkpoint pathway (NES = -2.169, adj.P < 0.001, FDR < 0.001) (**Figure 2(i)**). These results suggest that SLC7A11 may influence glioma progression through the regulation of metabolism, cell cycle, and immune-related pathways.

3.4. Correlation between SLC7A11 Expression and Glioma Immune Microenvironmen

ssGSEA immune infiltration analysis showed that SLC7A11 expression level was significantly correlated with infiltration scores of multiple immune cell types (**Figure 3(a)**). Specifically, it was significantly positively correlated with follicular helper T cells (TFH, R = 0.292, P < 0.001) (**Figure 3(b)**), central memory T cells (Tcm, R = 0.243, P < 0.001) (**Figure 3(c)**), and gamma-delta T cells (Tgd, R = 0.233, P < 0.001) (**Figure 3(d)**), and significantly negatively correlated with Th2 cells (R = -0.294, P < 0.001) (**Figure 3(e)**). These results suggest that SLC7A11

may be involved in regulating the glioma immune microenvironment and affect the immunosuppressive state.

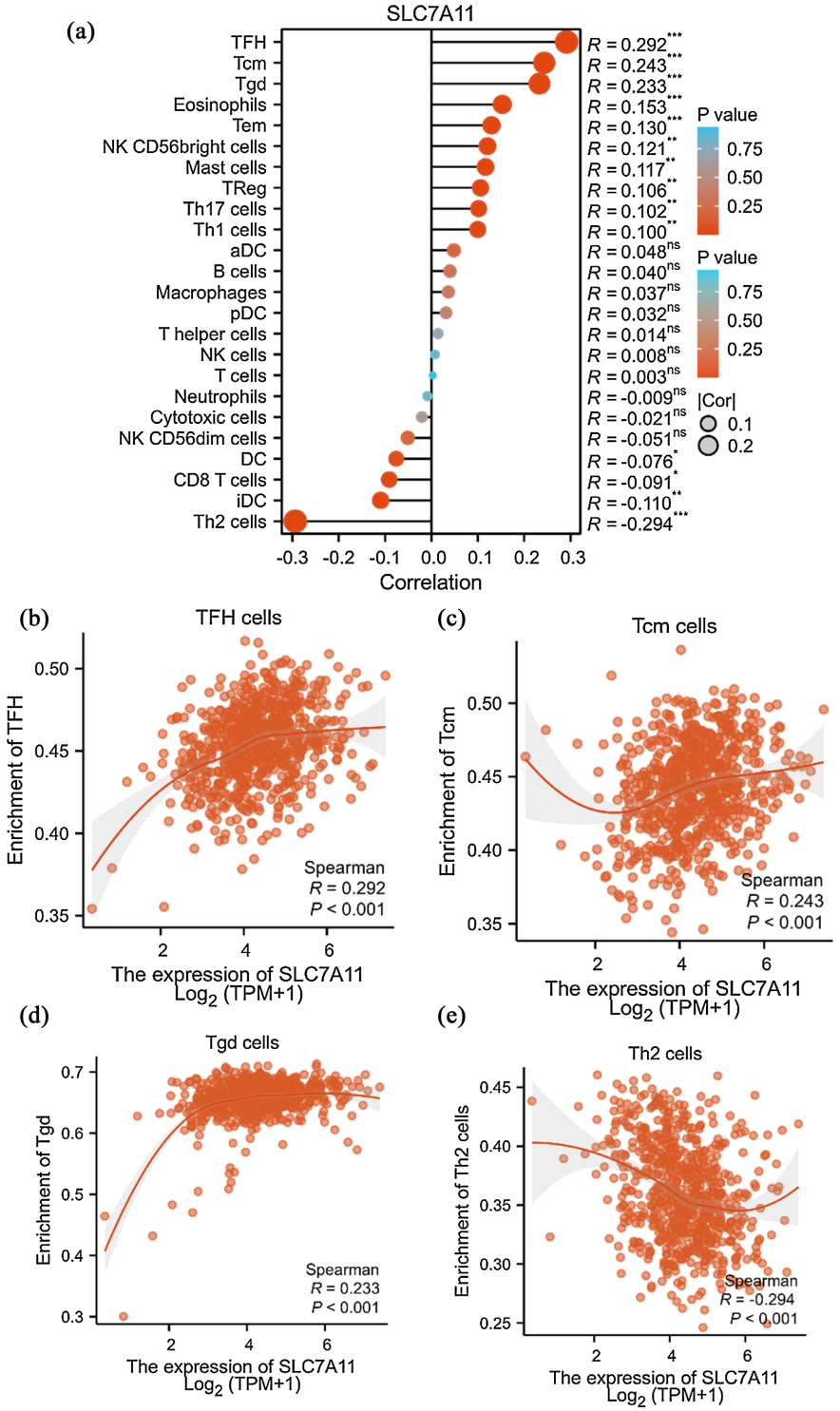

Figure 3. Correlation between SLC7A11 expression and glioma immune microenvironment. (a) Bubble plot of correlation between SLC7A11 expression and immune cell infiltration levels; (b) Scatter plot of SLC7A11 expression vs. TFH infiltration; (c) Scatter plot vs. Tcm; (d) Scatter plot vs. Tgd; (e) Scatter plot vs. Th2.

3.5. Relationship between SLC7A11 Expression and Prognosis of Glioma Patients

Kaplan-Meier survival analysis showed that patients in the high SLC7A11 expression group had significantly better overall survival (OS), disease-specific survival (DSS), and progression-free interval (PFI) than those in the low expression group (Figure 4). The log-rank test P values were 0.009 for OS, 0.044 for DSS, and 0.034 for PFI, indicating that high SLC7A11 expression is associated with a more favorable prognosis in glioma patients. Whole-cohort Kaplan-Meier survival analysis demonstrated that patients with high SLC7A11 expression had significantly superior OS, DSS, and PFI compared with the low expression group. However, given that high SLC7A11 expression is more prevalent in low-grade and IDH-mutant gliomas, this favorable prognostic association may be partly attributable to the unbalanced distribution of tumor grades and molecular subtypes. Because this study only performed whole-cohort survival analyses and did not conduct stratified survival analyses based on WHO pathological grade and IDH classification,

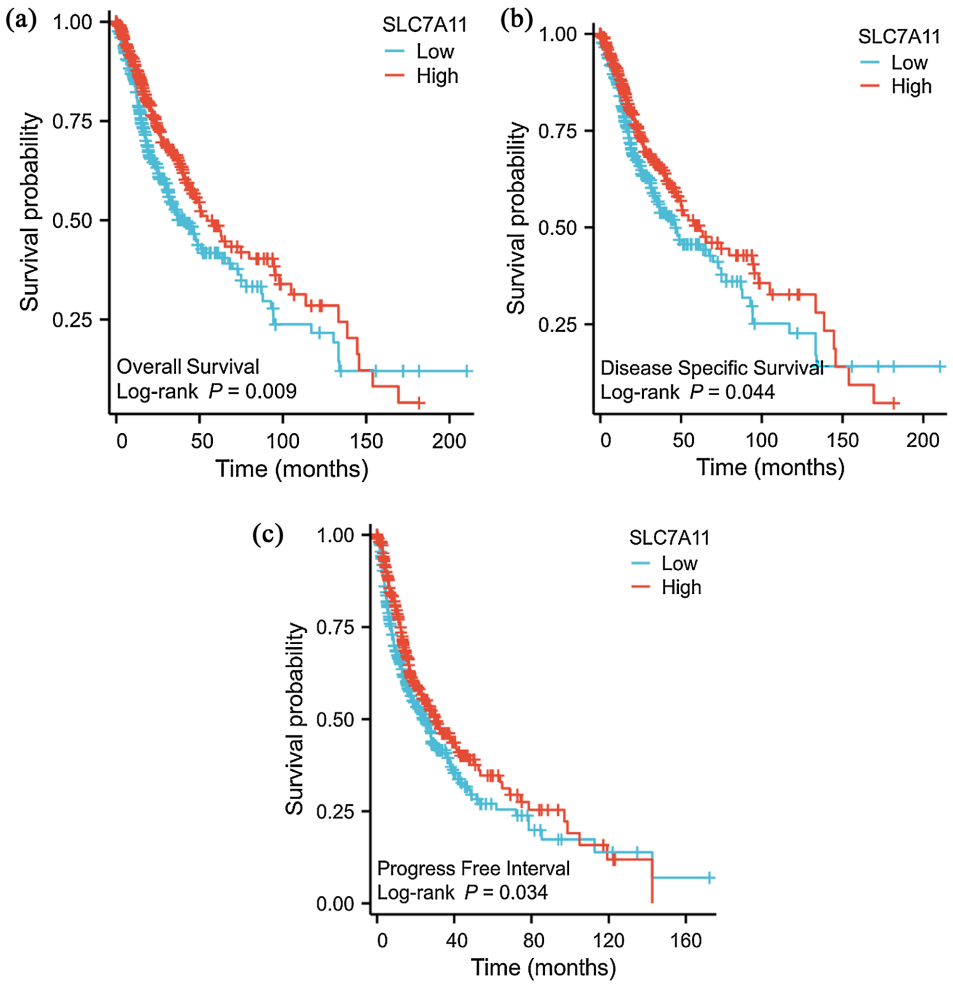

Figure 4. Relationship between SLC7A11 expression and prognosis of glioma patients. (a) OS curves for glioma patients with different SLC7A11 expression levels; (b) DSS curves; (c) PFI curves.

the confounding effect introduced by subtype compositional differences cannot be ruled out; relevant stratified validation remains to be addressed in future studies.

3.6. Independent Prognostic Factors for Glioma Patients and Nomogram Construction

Univariate Cox regression analysis showed that WHO grade (G3 vs. G2: HR = 2.967, 95% CI: 1.986 - 4.433, P < 0.001; G4 vs. G2: HR = 18.600, 95% CI: 12.448 - 27.794, P < 0.001), IDH mutation status (Mut vs. WT: HR = 0.116, 95% CI: 0.089 - 0.151, P < 0.001), age > 60 years (vs. ≤60 years: HR = 4.696, 95% CI: 3.620 - 6.093, P < 0.001), and SLC7A11 high expression (vs. low expression: HR = 0.728, 95% CI: 0.573 - 0.925, P = 0.010) were significantly associated with OS in glioma patients (Table 3). These variables were included in the multivariate Cox regression

Table 3. Univariate and multivariate Cox regression analysis of factors affecting overall survival in glioma patients.

Characteristics	Total (N)	Univariate analysis		Multivariate analysis	
		Hazard ratio (95% CI)	P value	Hazard ratio (95% CI)	P value
WHO grade	636				
G2	223	Reference		Reference	
G3	245	2.967 (1.986 - 4.433)	**<0.001**	2.051 (1.341 - 3.137)	**<0.001**
G4	168	18.600 (12.448 - 27.794)	**<0.001**	5.470 (3.251 - 9.203)	**<0.001**
IDH status	688				
WT	246	Reference		Reference	
Mut	442	0.116 (0.089 - 0.151)	**<0.001**	0.273 (0.187 - 0.400)	**<0.001**
Gender	698				
Female	297	Reference		Reference	
Male	401	1.250 (0.979 - 1.595)	0.073	1.242 (0.950 - 1.624)	0.114
Age	698				
≤60	555	Reference		Reference	
>60	143	4.696 (3.620 - 6.093)	**<0.001**	1.504 (1.112 - 2.034)	**0.008**
Race	685				
Asian	13	Reference			
Black or African American	33	1.578 (0.453 - 5.494)	0.473		
White	639	1.170 (0.374 - 3.657)	0.787		
SLC7A11	698				
Low	348	Reference		Reference	
High	350	0.728 (0.573 - 0.925)	**0.010**	1.105 (0.851 - 1.434)	0.455

Note: The original total number of cases was 699. Missing data were present in various clinical variables, and the complete-case method was adopted for the analysis, excluding samples with missing values for the corresponding indicator. Consequently, the Total (N) values differ across rows.

analysis. Results showed that WHO grade (G3 vs. G2: HR = 2.051, 95% CI: 1.341 - 3.137, P < 0.001; G4 vs. G2: HR = 5.470, 95% CI: 3.251 - 9.203, P < 0.001), IDH mutation status (Mut vs. WT: HR = 0.273, 95% CI: 0.187 - 0.400, P < 0.001), and age > 60 years (vs. ≤60 years: HR = 1.504, 95% CI: 1.112 - 2.034, P = 0.008) were independent prognostic factors for OS in glioma patients, whereas SLC7A11 expression level was not an independent prognostic factor (HR = 1.105, 95% CI: 0.851 - 1.434, P = 0.455).

Based on the multivariate Cox regression results, a nomogram combining WHO grade, IDH status, age, and SLC7A11 expression level was constructed to predict 1-, 3-, and 5-year OS probabilities in glioma patients (Figure 5(a)).

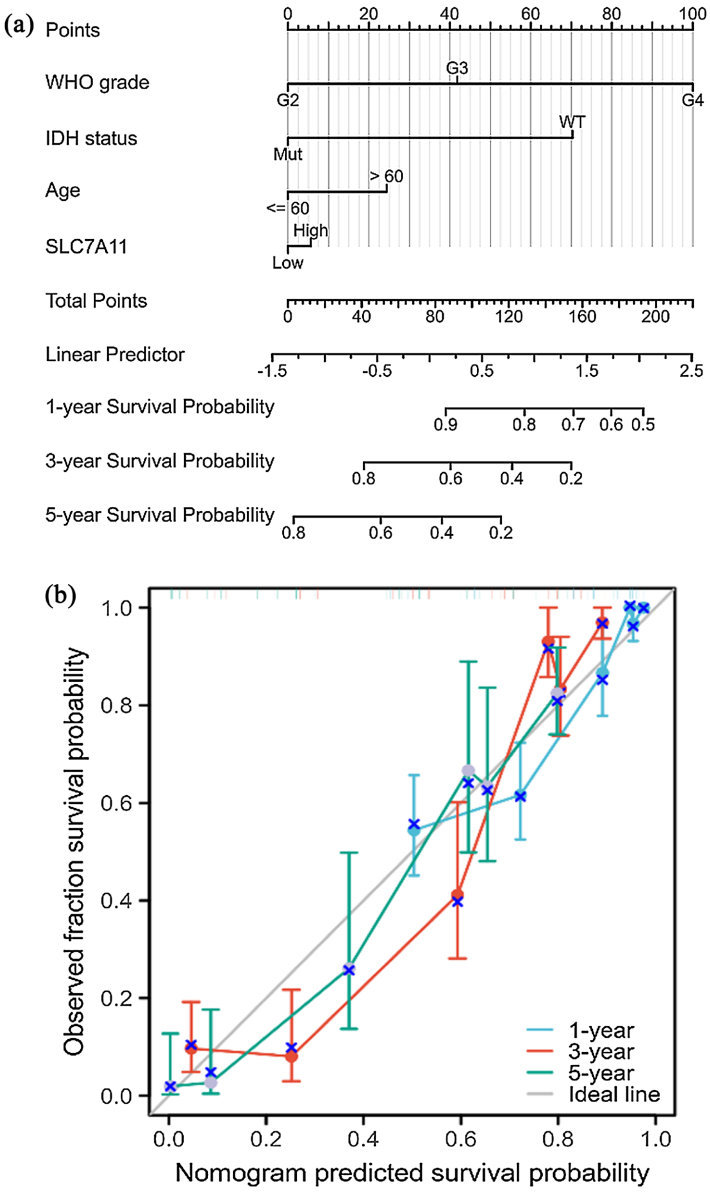

Figure 5. Independent prognostic factors for glioma patients and nomogram construction. (a) Nomogram constructed based on WHO grade, IDH status, age, and SLC7A11 expression level; (b) Calibration curves of the predictive nomogram.

Calibration curves showed good consistency between the nomogram-predicted survival probabilities and actual observed probabilities for 1, 3, and 5 years (**Figure 5(b)**), indicating favorable predictive performance of the model.

4. Discussion

Based on the TCGA and GTEx databases, this study systematically analyzed the expression characteristics, clinical associations, immune microenvironment, and prognostic value of SLC7A11 in glioma. The main findings include: SLC7A11 is expressed at significantly higher levels in glioma, yet its high expression is paradoxically associated with lower WHO grade, non-glioblastoma phenotype, and longer OS, DSS, and PFI; functional enrichment showed that the high-expression group was enriched in bile acid metabolism and KRAS signaling downregulation, whereas the low-expression group was enriched in EMT and cell cycle pathways; immune infiltration analysis revealed that SLC7A11 was positively correlated with TFH, Tcm, and Tgd, and negatively correlated with Th2 cells; the nomogram model constructed based on WHO grade, IDH status, age, and SLC7A11 demonstrated good survival predictive performance. The following discussion focuses on these key findings.

1) The "reverse" prognostic significance of SLC7A11 in glioma

Our finding that high SLC7A11 expression is associated with good prognosis contrasts with reports in most solid tumors (e.g., renal cell carcinoma, liver cancer) where it acts as an oncogenic marker [3] [12]. At the pan-cancer level, SLC7A11 promotes tumor progression by inhibiting ferroptosis [13]; however, our results suggest a non-canonical role in glioma. GSEA showed significant enrichment of KRAS signaling downregulation in the high-expression group, whereas the low-expression group was enriched for proliferation pathways such as MYC, E2F, and G2/M, providing molecular support for the indolent phenotype linked to high expression. Although SLC7A11 was not an independent prognostic factor in multivariate Cox regression, the nomogram combining it with strong factors like WHO grade and IDH status showed good calibration, suggesting that this molecule still has clinical integration value as a component of the model [14] [15].

2) Multidimensional association of SLC7A11 with the glioma immune microenvironment

Differential gene enrichment analysis showed that the genes distinguishing the SLC7A11 high- and low-expression groups were significantly enriched in immune pathways such as "immunoglobulin complex," "complement activation," and "neutrophil extracellular trap (NET) formation." This suggests that SLC7A11 may regulate the microenvironment by influencing humoral immunity and innate immunity. Previous studies have indicated that SLC7A11 can affect the functions of TAMs and T cells [16]; the present study extends these findings by revealing its association with B cells and NETs. Notably, we did not observe a significant negative correlation between SLC7A11 and $CD8^+$ T cell infiltration; instead, we found it to be negatively correlated with Th2 cells, while being positively correlated with TFH, Tcm, and Tgd. This immune landscape suggests that gliomas with high

SLC7A11 expression may present a microenvironment characterized by enhanced humoral immunity and immune memory, with attenuated Th2-type immunosuppression, thereby contributing to a favorable prognosis. In contrast, the relative enrichment of Th2 cells and iDCs in the low-expression group is associated with immunosuppression and tolerance, collectively constituting a tumor-promoting microenvironment.

3) Mechanistic interpretation of SLC7A11-related signaling pathways

Functional enrichment further revealed distinct signaling networks between the high- and low-expression groups. The high-expression group was enriched in the bile acid metabolism pathway, whereas the low-expression group was enriched in EMT, MYC targets, E2F targets, and G2/M checkpoint. As a cystine/glutamate antiporter, SLC7A11 promotes GSH synthesis and resistance to ferroptosis when highly expressed [17]; the enrichment of bile acid metabolism may represent a compensatory metabolic reprogramming that synergistically maintains redox homeostasis and supports a relatively "quiescent" cellular state. The activation of the EMT pathway in the low-expression group is consistent with its invasiveness and poor prognosis, while the significant enrichment of cell cycle checkpoints and MYC targets confirms that this tumor subtype is in a highly proliferative state [11]. Therefore, SLC7A11 may play a role as a molecular switch in glioma: its high expression anchors a low-grade malignant phenotype by inhibiting KRAS and proliferation pathways and promoting metabolic reprogramming, whereas its low expression releases the inhibition of EMT and the cell cycle, which is associated with tumor invasion and progression.

This study has several limitations: the data were sourced from retrospective public databases, making causal inference difficult; batch effects between TCGA and GTEx may have introduced bias; only mRNA levels were analyzed, lacking validation at the protein and post-translational modification levels; immune infiltration relied on algorithmic inference and requires validation by spatial transcriptomics or multicolor flow cytometry. Furthermore, stratified survival analyses by LGG/GBM and IDH mutant/wild-type subgroups were not conducted in this study; therefore, whether the prognostic advantage of SLC7A11 is universally applicable across subtypes remains unclear, which constitutes a limitation of the present work, and subsequent experiments will supplement stratified validation. Future studies should validate the nomogram in independent prospective cohorts and optimize the model by incorporating protein expression; utilize gene knockout/overexpression models combined with single-cell sequencing to elucidate the specific mechanisms by which SLC7A11 regulates KRAS, EMT, and NET formation; and explore whether combined therapeutic strategies targeting bile acid metabolism or NETs can remodel the immunosuppressive microenvironment of SLC7A11-low-expressing gliomas.

5. Conclusion

This study systematically demonstrated that SLC7A11 is highly expressed in gli-

oma yet significantly associated with low WHO grade, a non-GBM phenotype, and favorable prognosis, challenging the conventional view of SLC7A11 as an adverse prognostic marker in most solid tumors. Combined functional enrichment and immune infiltration analyses revealed that the high-expression group was enriched in bile acid metabolism and KRAS signaling downregulation, whereas the low-expression group exhibited activation of EMT and cell cycle pathways. Additionally, SLC7A11 was found to be positively associated with TFH, Tcm, and Tgd cells, and negatively associated with Th2 cells, suggesting a "low-invasive" microenvironment characterized by metabolic quiescence and retention of immune memory. The nomogram constructed based on WHO grade, IDH status, age, and SLC7A11 expression provides a well-calibrated novel tool for individualized prognostic prediction in glioma.

Conflicts of Interest

The authors declare no conflicts of interest regarding the publication of this paper.

References

[1] Sun, S., Guo, C., Gao, T., Ma, D., Su, X., Pang, Q., *et al.* (2022) Hypoxia Enhances Glioma Resistance to Sulfasalazine-induced Ferroptosis by Upregulating SLC7A11 via PI3K/AKT/HIF-1α Axis. *Oxidative Medicine and Cellular Longevity*, **2022**, Article ID: 7862430. https://doi.org/10.1155/2022/7862430

[2] Wang, J., Hao, S., Song, G., Wang, Y. and Hao, Q. (2023) The Prognostic and Clinicopathological Significance of SLC7A11 in Human Cancers: A Systematic Review and Meta-Analysis. *PeerJ*, **11**, e14931. https://doi.org/10.7717/peerj.14931

[3] Xu, F., Guan, Y., Xue, L., Zhang, P., Li, M., Gao, M., *et al.* (2021) The Roles of Ferroptosis Regulatory Gene SLC7A11 in Renal Cell Carcinoma: A Multi-omics Study. *Cancer Medicine*, **10**, 9078-9096. https://doi.org/10.1002/cam4.4395

[4] Wu, X., Wang, S. and Chen, K. (2023) Bulk RNA-Seq and scRNA-Seq Reveal SLC7A11, a Key Regulatory Molecule of Ferroptosis, Is a Prognostic-Related Biomarker and Highly Related to the Immune System in Lung Adenocarcinoma. *Medicine*, **102**, e34876. https://doi.org/10.1097/md.0000000000034876

[5] Ou, Y., Wu, N., Shu, L., Zhao, Y., Bao, Y. and Wu, Q. (2024) The High Expression of SLC7A11 and GPX4 Are Significantly Correlated with β-Catenin in Colorectal Cancer. *Cancer Management and Research*, **16**, 1639-1648. https://doi.org/10.2147/cmar.s483526

[6] Wang, Z., Wang, Y., Shen, N., Liu, Y., Xu, X., Zhu, R., *et al.* (2024) AMPKα1-Mediated ZDHHC8 Phosphorylation Promotes the Palmitoylation of SLC7A11 to Facilitate Ferroptosis Resistance in Glioblastoma. *Cancer Letters*, **584**, Article ID: 216619. https://doi.org/10.1016/j.canlet.2024.216619

[7] Zhao, X., Zhou, M., Yang, Y. and Luo, M. (2021) The Ubiquitin Hydrolase OTUB1 Promotes Glioma Cell Stemness via Suppressing Ferroptosis through Stabilizing SLC7A11 Protein. *Bioengineered*, **12**, 12636-12645. https://doi.org/10.1080/21655979.2021.2011633

[8] Yu, H., Zhu, K., Wang, M. and Jiang, X. (2023) TXNDC12 Knockdown Promotes Ferroptosis by Modulating SLC7A11 Expression in Glioma. *Clinical and Translational Science*, **16**, 1957-1971. https://doi.org/10.1111/cts.13604

[9] Tian, Q., Dan, G., Wang, X., Zhu, J., Chen, C., Tang, D., *et al.* (2025) IDO1 Inhibits Ferroptosis by Regulating FTO-Mediated M6a Methylation and SLC7A11 mRNA Stability during Glioblastoma Progression. *Cell Death Discovery*, **11**, Article No. 22. https://doi.org/10.1038/s41420-025-02293-3

[10] Wang, X., Yang, J., Yang, F. and Mu, K. (2023) The Disulfidptosis-Related Signature Predicts Prognosis and Immune Features in Glioma Patients. *Scientific Reports*, **13**, Article No. 17988. https://doi.org/10.1038/s41598-023-45295-w

[11] Luo, M., Liu, R., Li, Y., *et al.* (2023) Investigating the Prognostic Value of Constructing Disulfidptosis-Related Gene Models for Lung Adenocarcinoma Patients. *European Review for Medical and Pharmacological Sciences*, **27**, 9569-9585.

[12] Xu, B., Liang, J., Fu, L., Wei, J. and Lin, J. (2024) A Novel Oncogenic Role of Disulfidptosis-Related Gene SLC7A11 in Anti-Tumor Immunotherapy Response to Human Cancers. *Current Cancer Drug Targets*, **24**, 846-866. https://doi.org/10.2174/0115680096277818231229105732

[13] He, J., Ding, H., Li, H., Pan, Z. and Chen, Q. (2021) Intra-Tumoral Expression of SLC7A11 Is Associated with Immune Microenvironment, Drug Resistance, and Prognosis in Cancers: A Pan-Cancer Analysis. *Frontiers in Genetics*, **12**, Article 770857. https://doi.org/10.3389/fgene.2021.770857

[14] Liu, R., Wang, Y., Bu, J., Li, Q., Chen, F., Zhu, M., *et al.* (2024) Construction and Validation of Novel Ferroptosis-Related Risk Score Signature and Prognostic Prediction Nomogram for Patients with Colorectal Cancer. *International Journal of Medical Sciences*, **21**, 1103-1116. https://doi.org/10.7150/ijms.91446

[15] Zhao, G., Wu, Z., Ge, L., Yang, F., Hong, K., Zhang, S., *et al.* (2021) Ferroptosis-Related Gene-Based Prognostic Model and Immune Infiltration in Clear Cell Renal Cell Carcinoma. *Frontiers in Genetics*, **12**, Article 650416. https://doi.org/10.3389/fgene.2021.650416

[16] Jia, X., Shi, Y., Su, J., Zhou, Y., Li, W., Li, Y., *et al.* (2026) Amino Acid Transporter SLC7A11 Functions in Ferroptosis Regulation and Immune Microenvironment in Osteosarcoma. *International Immunopharmacology*, **168**, Article ID: 115876. https://doi.org/10.1016/j.intimp.2025.115876

[17] Park, J., Kilic, O., Deo, M., Jimenez-Cowell, K., Demirdizen, E., Kim, H., *et al.* (2023) CIC Reduces xCT/SLC7A11 Expression and Glutamate Release in Glioma. *Acta Neuropathologica Communications*, **11**, Article No. 13. https://doi.org/10.1186/s40478-023-01507-y